

Article

Influence of Glazed Hollow Bead on the Performance of Polyvinyl Alcohol Fiber Reinforced Cement Composites

Jie Dai ^{1,2}, Xuesen Li ^{1,*}, Yadi Zhao ¹ and Yunfei Li ¹

¹ School of Civil Engineering, Henan University of Technology, Zhengzhou 450001, China; daijie@haut.edu.cn (J.D.); liuqiang@haut.edu.cn (Y.Z.); xuqikeng@haut.edu.cn (Y.L.)

² Henan Key Laboratory of Grain and Oil Storage Facility & Safety, Henan University of Technology, Zhengzhou 450001, China

* Correspondence: zjq986@haut.edu.cn; Tel.: +86-186-2371-3078

Abstract: To improve the thermal insulation properties and toughness of concrete, the glazed hollow bead (GHB) and polyvinyl alcohol (PVA) fiber reinforced cementitious composites (GPCC) were investigated by orthogonal test, which includes six GHB mass percentage (20%, 40%, 60%, 80%, 100%, 120%), three PVA volume fraction (1%, 1.5%, 2%) and water binder ratio (0.26, 0.30, 0.34). Compressive, split tensile strengths and thermal conductivity of GHB-PVA reinforced cementitious composites (GPCC) were tested, and the mechanism of fibers was analyzed from a microscopic perspective. The results revealed that the thermal insulation will be significantly improved with the increased content of GHB, but the compressive and split tensile strength will be decreased simultaneously. No obvious effect was found by the PVA fiber addition on its strength indexes, and the presence of GHB will affect the bridging action of PVA fibers. The water binder ratio has more effect on strengths than thermal conductivity. Based on the mechanical performance rather than the thermal insulation analysis test, the optimal mix proportions were proposed: mass percentage of 40% GHB, a volume fraction of 1.5% PVA fiber, and 0.26 water-binder ratio. Moreover, the anchoring and bridging effect of PVA fibers will effectively balance the stress generated by the shrinkage of cement paste, and inhibits or even prevents the development of cracks. However, a certain number of tiny cracks will be formed near the GHB, and between GHB and PVA fibers, which will cause local stretching and peeling of PVA, and shattering inside the GHB with the increase of external force. The findings of this study can provide a useful reference for the application of an insulated-bearing material with GHB and PVA fiber.

Keywords: polyvinyl alcohol fiber; glazed hollow bead; mechanical properties; thermal conductivity; micro-structure



Citation: Dai, J.; Li, X.; Zhao, Y.; Li, Y. Influence of Glazed Hollow Bead on the Performance of Polyvinyl Alcohol Fiber Reinforced Cement Composites. *Crystals* **2022**, *12*, 454. <https://doi.org/10.3390/cryst12040454>

Academic Editors: Yang Yu, Weiqiang Wang, Rafael Shehu, Beatrice Pomaro and José L. García

Received: 15 February 2022

Accepted: 22 March 2022

Published: 24 March 2022

Publisher's Note: MDPI stays neutral with regard to jurisdictional claims in published maps and institutional affiliations.



Copyright: © 2022 by the authors. Licensee MDPI, Basel, Switzerland. This article is an open access article distributed under the terms and conditions of the Creative Commons Attribution (CC BY) license (<https://creativecommons.org/licenses/by/4.0/>).

1. Introduction

The subject of energy conservation in buildings has become one of most important at present. With urbanization and increasing population, the energy consumption of buildings has reached 40% of the overall energy consumption worldwide [1,2]. Additionally, the global building sector has contributed 28% of global energy-related to CO₂ emissions [3]. Recently, measures of energy conservation in building were proposed for mitigating global warming caused by increased energy consumption and carbon use, in order to reduce the greenhouse gas emissions by 2030, which is in accordance with the Paris Agreement [4]. A large part of the energy consumption is related to heating and cooling of buildings [5,6]. Using the thermal performance of building materials to passively reduce thermal convection between the interior and exterior is considered to be the most effective way to save energy.

In terms of thermal insulation composites, cementitious materials containing GHB were explored extensively. GHB has a special structure with a closed surface and a hollow interior, and it has excellent characteristics of low density, low thermal conductivity, high temperature resistance, low water absorption, etc., which is a good choice to improve

the thermal insulation performance of building materials. Studies have shown that the addition of appropriate amounts of glass beads to concrete can effectively improve the thermal insulation capacity of the material, the workability of the mix, and reduce its apparent density [7]. Zhao, et al. studied the effect of GHB particle admixture (6–12%) on the mechanical properties and thermal conductivity of concrete, and found that as the admixture of GHB increased from 6% to 12%, the compressive strength of concrete decreased by 1.5% and the thermal conductivity decreased by 17.5% [8,9]. Liu J. Y. [10] et al. conducted an experimental study and numerical analysis on the seismic performance [11] and thermal performance [12] of glass bead insulated concrete beams [13] and shear walls, and the load bearing capacity and damage mode of glass bead concrete members are basically the same as those of ordinary concrete, but glass bead insulated concrete can effectively prevent heat intrusion [14], which not only has a significant protective effect on reinforcement [15], but can also reduce the indoor temperature variation of buildings in winter and summer seasons to meet the requirements of comfort [16].

However, because the glass beads have a spherical shape on the outer surface, they are easily broken by extrusion and vibration in the concrete mixing process, resulting in strength loss. Additionally, the concrete with glass beads can very easily suffer brittle damage [7,14]. Wu, et al. designed a single-factor test to analyze the effects of different glass bead dosages (38.4%, 41.6%, 42.7%, 43.8%, 46.1%) on the insulation mortar. It was found that the 28 days compressive strength increased (increased by 14%) and then decreased (decreased by 5%) with the increase of glass beads dosage, mainly because the compressive strength decreased due to the reduction of powder after the dosage of glass beads exceeded 45% [17]. As indicated above, insulation cementitious materials containing GHB are generally able to ensure strength and at the same time have good insulation properties. However, there is the possibility of brittle damage, which limits its application

To overcome the brittleness of concrete, adding the right amount of uniform anisotropic distribution of fibers in concrete becomes an effective way to improve the toughness of concrete. It has been shown that fiber concrete has good tensile and shear properties and can be used in engineering fields, such as repair and restoration of bridge deck slabs [18] and design of new frame nodes [19]. Additionally, in order to improve the brittle damage mode of concrete materials through the good crack arresting effect of fibers and to improve the seismic performance and damage resistance of structural members, V.C. Li et al. introduced polyvinyl alcohol (PVA) fibers into engineered cementitious composites [20]. In similar studies, polyvinyl alcohol (PVA) fibers at a volume fraction of 2% added to engineered cementitious composites, can achieve a tensile strain capacity up to 3–5%, approximately 500 times larger than that of normal concrete or fiber reinforced concrete [21,22]. Amin Al-Fakih et al. investigated the effect of PVA fibers on the flexural and tensile strengths of engineered cementitious materials. The result showed that the flexural strength of specimens with 0.5% and 2.0% PVA fiber was enhanced by more than 40% and 55%, and the tensile strength of the specimens with 1.25% and 2.0% PVA fiber improved by 31% and 61% [23,24]. Huang found through the study of the performance of PVA fiber concrete, that the incorporation of PVA fiber to a certain extent can strengthen the compressive, flexural, and split strength of concrete; the highest growth rates compared to the base concrete: 17.71%, 16.04%, and 37.44%, respectively [25].

Most of the existing studies focus on GHB insulating concrete and fiber concrete, but there are relatively few studies on fiber-glass bead cementitious composites. Zhu J. et al. [16,26] conducted experimental studies on the basic mechanical properties, dry shrinkage cracking properties of polypropylene fiber glass bead composite insulation mortar, and obtained that polypropylene fiber can inhibit the development rate of dry shrinkage cracking of glass bead insulation mortar and improve the flexural strength of glass bead composite insulation material [27]. Xu J. W. et al. [28] showed that the effect of steel fibers on the compressive strength of insulating concrete was small, but could increase its tensile strength by 88.44%. Wang C. G. [29] mixed PVA with expanded vitrified small balls in foam concrete, which not only improved its mechanical properties significantly, but was also able to limit the

development of cracks in the foam concrete matrix and pore wall cracks, and reduce the water absorption and thermal conductivity of foam concrete [30].

To meet the requirements of energy saving and green development, a novel material with great heat insulation, load-bearing performance, and crack resistance for buildings, especially for special structures (such as storage structures), is needed. The former research and references have verified that the addition of PVA fiber can improve the concrete toughness excellently. Therefore, orthogonal tests were designed with the factors of GHB content, PVA fiber content, and water-binder ratio to investigate the mechanical and thermal performance of GPCC. Additionally, the micro-structure of the specimens was observed by SEM to explore the action of GHB and PVA fiber. This study provides a basis for further research on the application of GPCC and proposes an optimized mix proportion.

2. Experimental Programs

2.1. Materials

The test was conducted using P-O 42.5 grade ordinary silicate cement produced by Xinxiang Nova, Xinxiang, China, which has a 28 days compressive strength of 48.3 MPa. The I grade fly ash produced by a power plant was used. Natural river sand with a maximum particle diameter of 1.18 mm is used for fine aggregates. The fibers are made of polyvinyl alcohol fibers (PVA) from Kuraray, Tokyo, Japanese, their appearance and SEM image are shown in Figure 1 and the parameters are shown in Table 1. The GHB was produced by Hebei Yixin Building Material Technology Co., Ltd., Hengshui, China, its appearance and SEM image are shown in Figure 1, and the performance indexes are shown in Table 2. The AEWR air-entraining water reducer with a water reduction rate of 15% was used as the water reducer.

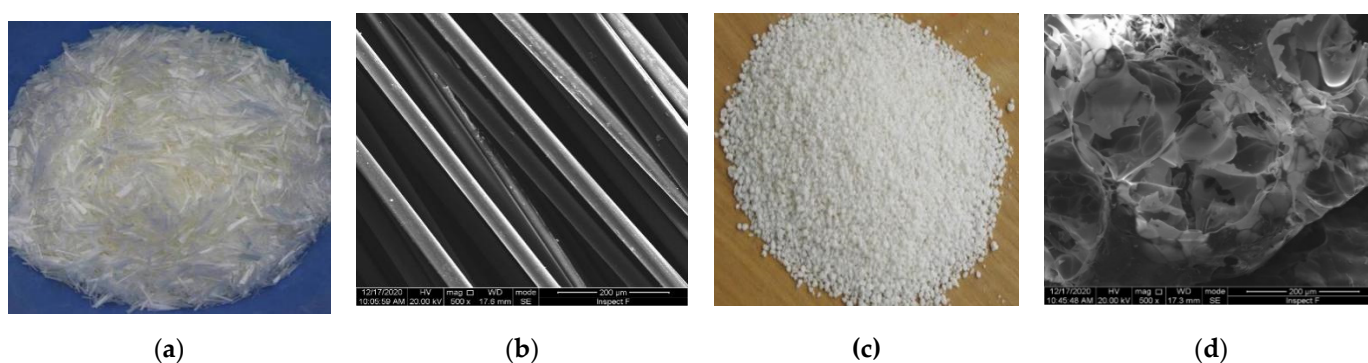


Figure 1. Materials: (a) PVA fibers; (b) SEM image of PVA fiber; (c) GHB; (d) SEM image of GHB.

Table 1. The properties of PVA fiber.

Length (mm)	Diameter (μm)	Tensile Strength (MPa)	Elastic Modulus (GPa)	Elongation (%)	Density (g/cm^3)
12.8	39	1600	40	7	1.3

Table 2. The properties of GHB.

Particle Size (mm)	Bulk Density ($\text{kg}\cdot\text{m}^{-3}$)	Thermal Conductivity ($\text{W}/(\text{m}\cdot\text{K})$)	Refractory Temperature ($^{\circ}\text{C}$)	Cylinder Compressive Strength (Volume Loss Rate at 1 MPa Pressure)	Water Absorption (%)
0.5–1.5	80–130	0.032–0.045	1280–1360	38–46%	20–50

2.2. Orthogonal Experimental Design

It has been shown that the water-binder ratio is the main factor affecting the mechanical properties of concrete, the PVA fiber content mainly improves the toughness of concrete, and the porosity and particle characteristics of lightweight fine aggregates are the main factors affecting the thermal conductivity of concrete. Therefore, with the background of a reserve grain depot project demand in Lanzhou City, according to the GPCC pre-testing results, this test was performed according to the orthogonal design table $L_{18} (6^1 \times 3^2)$ of three factors and mix levels. GHBs are used in place of fine aggregates; the PVA fiber content, GHB content, and water-binder ratio were selected as the influencing factors of the orthogonal test. Eventually the volume percentage of GHB was designed as factor A with six levels (20%, 40%, 60%, 80%, 100%, 120%), the PVA fiber fraction was designed as factor B with three levels (1.0%, 1.5%, 2.0%), and three water-binder ratio levels of 0.26, 0.3, and 0.34 were designed as factor C in this experiment. The factors and the levels of the orthogonal experiment are shown in Table 3. The mix proportions and test results are shown in Table 4.

Table 3. Factor and level of the orthogonal experiments.

Factor		Lever					
		1	2	3	4	5	6
A	GHB	20%	40%	60%	80%	100%	120%
B	PVA	1.0%	1.5%	2.0%			
C	Water-binder ratio	0.26	0.3	0.34			

Table 4. Mix proportions and test results.

Test No	A	B	C	Fly Ash	Cement	Sand	Compressive Strength (MPa)	Split Tensile Strength (MPa)	Thermal Conductivity (W/(m·K))
	GHB (%)	PVA (%)	Water						
1	20	1.0	0.34	0.5	0.5	0.36	24.63	3.73	0.8967
2	20	1.5	0.26	0.5	0.5	0.36	36.33	5.20	0.8714
3	20	2.0	0.30	0.5	0.5	0.36	30.23	4.60	0.8532
4	40	1.0	0.30	0.5	0.5	0.36	29.57	5.40	0.7399
5	40	1.5	0.34	0.5	0.5	0.36	26.17	4.03	0.7571
6	40	2.0	0.26	0.5	0.5	0.36	31.63	4.10	0.7643
7	60	1.0	0.26	0.5	0.5	0.36	31.30	3.68	0.7447
8	60	1.5	0.30	0.5	0.5	0.36	36.80	3.87	0.6748
9	60	2.0	0.34	0.5	0.5	0.36	20.77	2.80	0.7145
10	80	1.0	0.26	0.5	0.5	0.36	20.90	3.47	0.6517
11	80	1.5	0.30	0.5	0.5	0.36	25.53	3.42	0.6351
12	80	2.0	0.34	0.5	0.5	0.36	17.10	2.77	0.6300
13	100	1.0	0.30	0.5	0.5	0.36	13.77	2.73	0.6305
14	100	1.5	0.34	0.5	0.5	0.36	22.63	2.67	0.6733
15	100	2.0	0.26	0.5	0.5	0.36	25.90	4.00	0.7651
16	120	1.0	0.34	0.5	0.5	0.36	17.10	2.43	0.7060
17	120	1.5	0.26	0.5	0.5	0.36	17.70	3.40	0.6555
18	120	2.0	0.30	0.5	0.5	0.36	17.13	3.47	0.7864

2.3. Specimens Preparation

This test adopts forcing mixer to mix GPCC. Firstly, the feeding order is to put in cement, fly ash, sand, and GHB and mix well. Then the water reducing agent and water are evenly mixed and put into the mixture and stirred well. Finally, PVA fiber is added and mixing is continued, in order to create a mixture with good fluidity, fiber stirring without obvious agglomeration phenomenon, regarded as uniform mixing. The test blocks were cast in plastic test molds, vibrated, and compacted by shaking table, covered with cling film for 36 h and demolded, and maintained under standard maintenance conditions (relative

humidity $\geq 95\%$, temperature 20 ± 1 °C) for 28 days, taken out and dried for the test of mechanical properties and thermal conductivity.

2.4. Test Methods

The compressive, split strengths, and thermal conductivity of GPCC were tested, and the microstructure images were observed. They are briefly described below.

2.4.1. Strength Test

The compressive strength and split tensile test were conducted in accordance with the “Standard for Test Method of Mechanical Properties on Ordinary Concrete” (GB/T 50081-2019, Chinese standard) [31] using a JYE-2000A type fully-automatic constant-pressure pressure testing machine (see Figure 2a,b) which produced by Beijing Ouya Zhongxing Science Co., Ltd., Beijing, China. The $100 \times 100 \times 100$ mm³ specimens were prepared to measure the compressive and split tensile strengths. As per the standards, the rate of loading should be controlled for 3 mm/min in the compressive strength and split tensile strength tests.

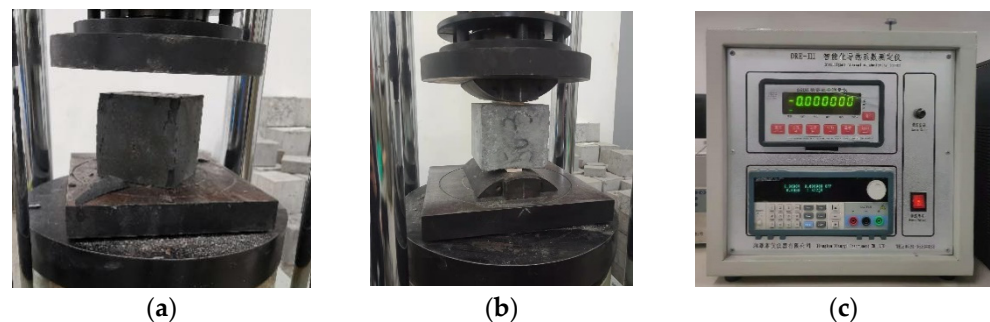


Figure 2. The test apparatus and loading: (a) compressive strength; (b) split tensile strength; (c) thermal conductivity.

2.4.2. Thermal Conductivity Test

The thermal conductivity of the GPCC was tested using the “Standard for thermal insulation -Determination of steady-state thermal resistance and related properties -Heat flow meter apparatus” (GB10295-2008, Chinese standard) [32] with a DRE-III multifunctional rapid thermal conductivity testing machine (see Figure 2c) which produced by Xiangtan Xiangyi instrument Co., Ltd., Xiangtan, China. The $300 \times 300 \times 10$ mm³ specimens were prepared to measure the thermal conductivity. As per the standards, the temperature of the hot side is set on the hot plate side of the instrument and the heat is transferred through the sample to the cold side which is at room temperature, and the heat flow transfer is measured by this method. Finally, the thermal conductivity of the GPCC is calculated based on the thickness and heat transfer area of the sample.

2.4.3. Scanning Electron Microscope Test

The micro-structure of the specimen was observed using a scanning electron microscope (FEI INSPECT, F50) which produced by FEI company, Hillsboro, OR, USA. The samples were taken from the test cubes used in the axial compression test, which had a diameter of 4 mm and a thickness of 2 mm. To observe the microscopic morphology of the GHB and the PVA fibers in the concrete, the sample was taken without any coarse aggregate.

3. Results and Discussion

3.1. Analysis of Range

Range analysis will intuitively show the order of each factor’s influence on the evaluation index, which is presented in Table 5 and Figure 3.

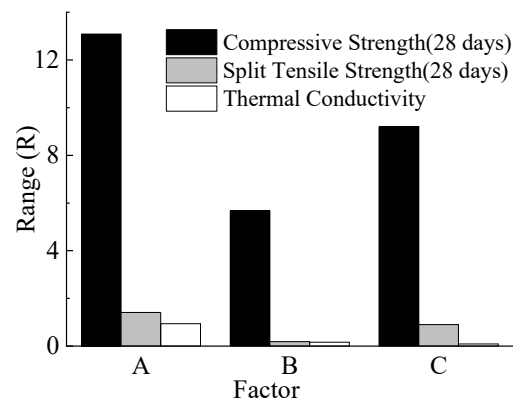


Figure 3. Range chart.

Table 5. Analysis results of range.

Number	Compressive Strength (MPa)			Split Tensile Strength (MPa)			Thermal Conductivity (W/(m·K))		
	A	B	C	A	B	C	A	B	C
K ₁	91.20	137.27	163.77	13.53	21.45	23.85	2.6213	4.3696	4.4527
K ₂	87.37	165.17	153.03	13.53	22.59	23.49	2.2613	4.2671	4.3199
K ₃	88.87	142.77	128.40	10.35	21.73	18.43	2.1340	4.5135	4.3776
K ₄	63.53			9.65			1.9168		
K ₅	62.30			9.40			2.0688		
K ₆	51.93			9.30			2.1479		
K ₁	30.40	22.88	27.30	4.51	3.57	3.97	0.8738	0.7283	0.7421
K ₂	29.12	27.53	25.51	4.51	3.77	3.92	0.7538	0.7112	0.7200
K ₃	29.62	23.80	21.4	3.45	3.62	3.07	0.7113	0.7522	0.7296
K ₄	21.18			3.22			0.6389		
K ₅	20.77			3.13			0.6896		
K ₆	17.31			3.10			0.7160		
R	13.09	5.68	9.21	1.41	0.19	0.90	0.2348	0.0411	0.0221

Note: The number after the letter represents the corresponding level of each factor. K_i represents the sum of the experimental results corresponding to the level value of i in any column of factors.

For compressive strength of GPCC, the affecting ranking is GHB content (A) > water-binder ratio (C) > PVA fiber content (B), indicates that the influence of GHB content is most obvious. As shown in Figure 4a, the compressive strength decreased with the increase of GHB. This is due to the porous cavity structure inside the GHB, and its cylinder compressive strength is lower than that of the matrix, which makes it easy to form penetration joints inside the composite material when it is compressed, accelerating the destruction of the material and leading to the reduction. When the amount of GHB is more than 60%, the breakage rate increases due to the collision between GHB and other materials in the mixing process, which causes the compressive strength dropped significantly. Then, as the main factor affecting the matrix compactness, the effect of water-binder ratio on the compressive strength of GPCC is obvious too, as shown in Figure 4c. Meanwhile, the effect of fiber content is not obvious because the fiber content has little effect on the compactness of the matrix, as shown in Figure 4b. Additionally, the optimal solution is: A1-B3-C1.

For split tensile strength, the affecting ranking is: water-binder ratio (C) > GHB content (A) > PVA fiber content (B), as shown in Figure 5. The effect of water-binder ratio and GHB content is more obvious. Especially for large amounts of GHB (more than 60%), the split tensile strength will decrease rapidly. GHB will reduce the inhibitory effect of fibers on the development of internal pores and micro-cracks in composite. The optimal solution is: A1-B2-C1.

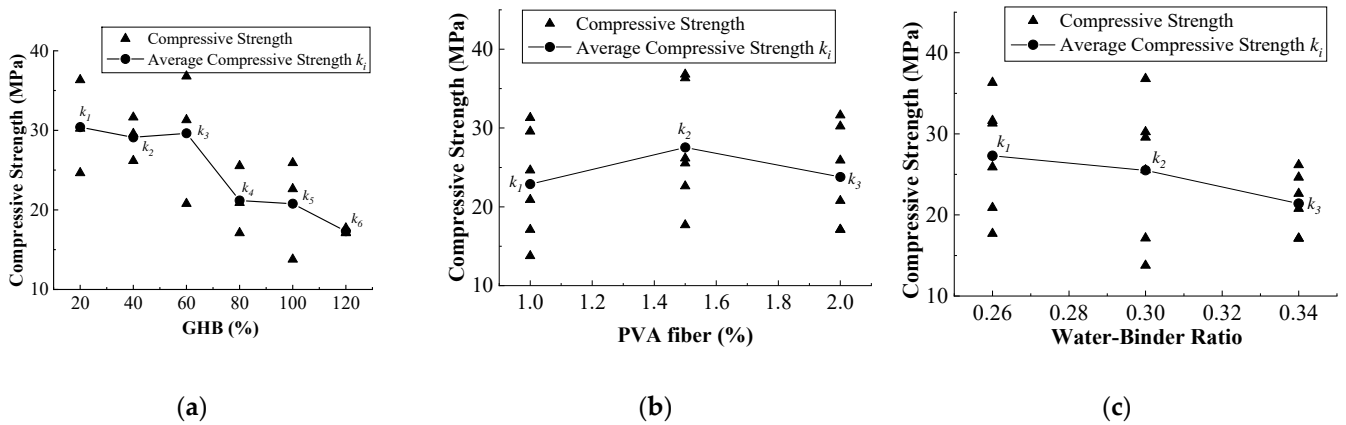


Figure 4. Relationship of GPCC compressive strength with each factor: (a) GHB content; (b) PVA fiber content; (c) water-binder ratio.

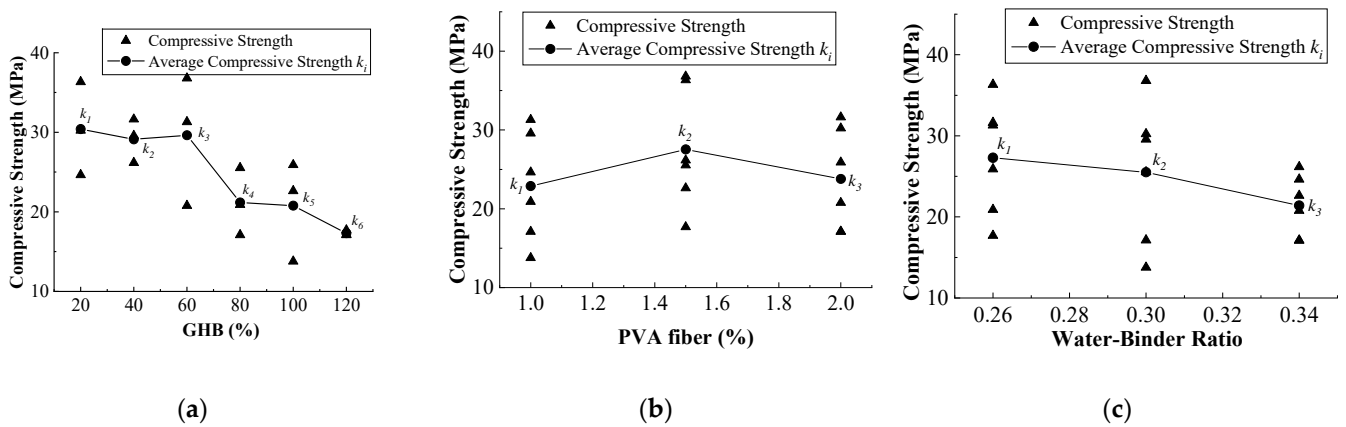


Figure 5. Relationship of GPCC split tensile strength with each factor: (a) GHB content; (b) PVA fiber content; (c) water-binder ratio.

For thermal conductivity, the affecting ranking is: GHB content (A) > PVA fiber content (B) > water-binder ratio (C). As shown in Figure 6a, the GPCC thermal conductivity decreases and then increases with the increase of GHB, indicating that the reduction effect of GHB on the thermal conductivity of the composite reaches the limit when its dosing is about 80%. With the increase of GHB amount, the content of cement paste in the composite material per unit volume is relatively reduced, and when it is reduced to a limit value, a large number of connected pores and channels from the inside to the surface of unfilled GHB appear in the composite material, so that the closed pore voids are relatively reduced, and then the thermal conductivity will rise. As shown in Figure 6b,c, the fiber content has some effect on the thermal conductivity of GPCC, and the water-binder ratio has the least effect on the thermal conductivity. The optimal solution is: A4-B2-C2.

Based on the range analysis, the content of GHB has the most important influence on the mechanical properties and thermal insulation of GPCC, and the water-binder ratio mainly affects the strength of GPCC by the influence on its matrix. However, the effect of PVA fiber was less than the other factors.

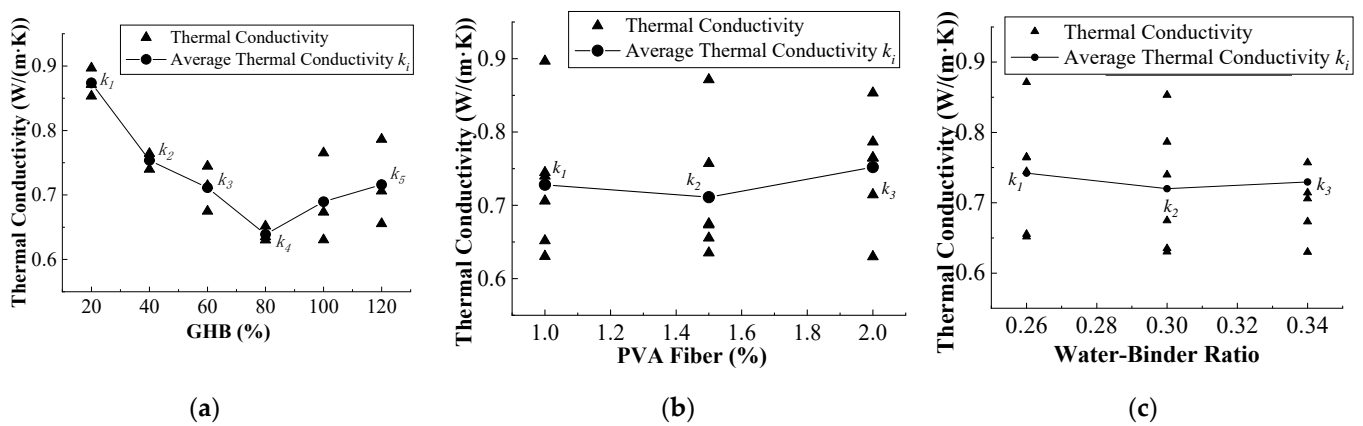


Figure 6. Relationship of GPC thermal conductivity with each factor: (a) GHB content; (b) PVA fiber content; (c) water-binder ratio.

3.2. Variance Analysis

To estimate the importance of each factor more precisely, the results were analyzed by variance analysis in Tables 6–8, to find the mean square value and F-value of each factor.

GHB content has a significant effect on the compressive strength of GPC, water-binder ratio and GHB contents have significant effect on the split strength of GPC, and the influence of GHB content is significant for thermal conductivity of GPC. As observed, the results are in accordance with range analysis. Although the addition of GHB can play a positive role in improving the thermal insulation performance of GPC, the high addition of GHB will reduce the strength of GPC. When the amount of GHB addition is more than 60%, the compressive strength will drop sharply, and when the amount of GHB added is more than 40%, the split tensile strength will drop sharply. The most significant effect of water–cement ratio on tensile split strength, and the split tensile strength of GPC, can reach high values at low water to glue ratio. The fiber content had little effect on the strength and thermal conductivity of GPC, especially the split tensile strength.

Table 6. Variance analysis results of compressive strength.

Factors	Compressive Strength				
	SS	Df	MS	F	Significance
GHB	476.22	5	95.24	5.12	*
PVA fiber	72.80	2	36.40	1.96	-
Water-binder ratio	109.60	2	54.80	2.95	-
Intra-group errors	148.82	8	18.60	-	-
Sum	807.52	17	205.04	-	-

Note: “*” represents a significant effect of this factor on the results.

Table 7. Variance analysis results of split tensile strength.

Factors	Split Tensile Strength				
	SS	Df	MS	F	Significance
GHB	6.84	5	1.37	5.89	*
PVA fiber	0.12	2	0.06	0.25	-
Water-binder ratio	3.06	2	1.53	6.58	*
Intra-group errors	1.86	8	0.23	-	-
Sum	11.87	17	3.19	-	-

Note: “*” represents a significant effect of this factor on the results.

Table 8. Variance analysis results of thermal conductivity.

Factors	Thermal Conductivity				
	SS	Df	MS	F	Significance
GHB	0.09510	5	0.01902	9.76039	**
PVA fiber	0.00510	2	0.00255	1.30973	-
Water-binder ratio	0.00148	2	0.00074	0.37972	-
Intra-group errors	0.01559	8	0.00195	-	-
Sum	0.11727	17	0.02426	-	-

Note: "***" represents a high significant effect of this factor on the results.

3.3. Determination of the Optimum Proportion

The comprehensive balance method was used to analyze the influence of various factors on the performance indexes of GPCC, and finally obtain the optimum proportion. In Figures 4–6, k_i represents the arithmetic mean of the experimental results obtained when each factor was taken at level i .

The effect of GHB content (A) on each index can be obtained from Figure 3. The influence of A on compressive strength and thermal conductivity is ranked first and is the leading factor, and the influence on split tensile strength is ranked 2nd and is an important factor. From Figures 4–6, it can be observed that when taking k_2 , GPCC split tensile strength index is the best and compressive strength is basically the same as when taking the maximum index value, thus k_2 is taken. When k_3 is taken, compared with k_2 , GPCC compressive strength increases by 1.72%, GPCC thermal conductivity decreases by 5.64%, PEEC split strength decreases by 23.5%; when k_1 is taken, compared with k_2 , GPCC compressive strength increases by 4.40%, GPCC thermal conductivity increases by 15.92%, GPCC split strength is the same as that when k_2 is taken; when k_4 is taken, the thermal conductivity coefficient is the smallest, but the other three index values are relatively low, thus they are not considered. Combined with the above analysis, the A factor levels are taken as k_2 .

The effect of PVA fiber content (B) on each index can be obtained from Figure 3: B is the second most important factor for the effect on thermal conductivity, and the third most important factor for split tensile strength and compressive strength. From Figures 4–6, the compressive strength, split tensile strength, and thermal conductivity of PEEC obtain the best index at all k_2 , thus the B factor levels are chosen as k_2 .

The effect of water-binder ratio (B) on each index can be obtained from Figure 3. Its influence on compressive strength and tensile strength ranks 2nd and is an important factor, while the influence on thermal conductivity ranks 3rd and is a minor factor. From Figures 4–6, the compressive strength and tensile strength are maximum when k_1 is taken, and the change of water-binder ratio has no effect on the thermal conductivity (compared with the best index k_2 , which is increased by 3%). Therefore, the C factor levels are chosen as k_1 .

Comprehensive analysis of the above, the optimal ratio for this test is A2-B2-C1, namely, 40% GHB, 1.5% PVA fiber, and 0.26 water-cement ratio.

3.4. Micro-Mechanical Analysis

Discontinuities and micro-cracks within conventional concrete are often weak points. PVA fibers can be used as a joining material to bridge discontinuous areas, not only to reduce discontinuities and micro-cracks within the concrete, but also as a bonding base for the cement. The hydration products from the hydration process are continuously gathered and bonded on the surface of the fiber to fill the gap between the fiber and the substrate, and to strengthen the weak points. As shown in Figure 7, the micro-structure of PVA fiber-reinforced concrete has a three-dimensional mesh distribution of fibers within the matrix. By means of the anchoring effect and bridging effect, it effectively balances the

stress generated by the shrinkage of cement paste, reduces the cracks caused by shrinkage, and inhibits or even prevents the development of cracks.

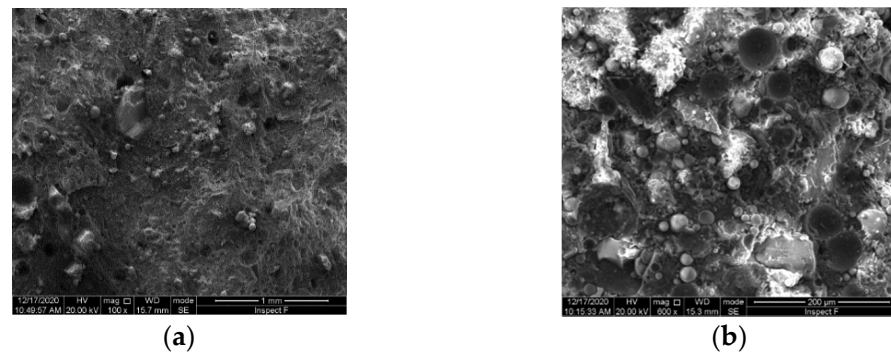


Figure 7. Micro-structure of GHB concrete and plain concrete: (a) GHB concrete; (b) plain concrete.

The area around the crack of the GPCC compressive specimen was cut and sampled, and the morphology of GPCC after compressive damage was observed by SEM electron microscopy as indicated in Figure 8. PVA fibers are randomly and evenly distributed in the cement matrix, forming a “skeleton” that can effectively disperse the stress and prevent the settlement and cracks of GHB. When macro cracks are created, the fibers can consume some of the energy used to create the cracks, weakening the stress concentration at the crack tip and impeding the growth and development of the cracks. However, a certain number of tiny cracks will be formed near the GHB, near the fibers, and between the GHB and the fibers. With the increase of external force, these tiny cracks will extend along the matrix to the interface of fiber, GHB, and hydration products, or even penetrate the fiber and GHB, causing local stretching and peeling of PVA fibers and shattering inside the GHB, which will lead to the destruction of the material.

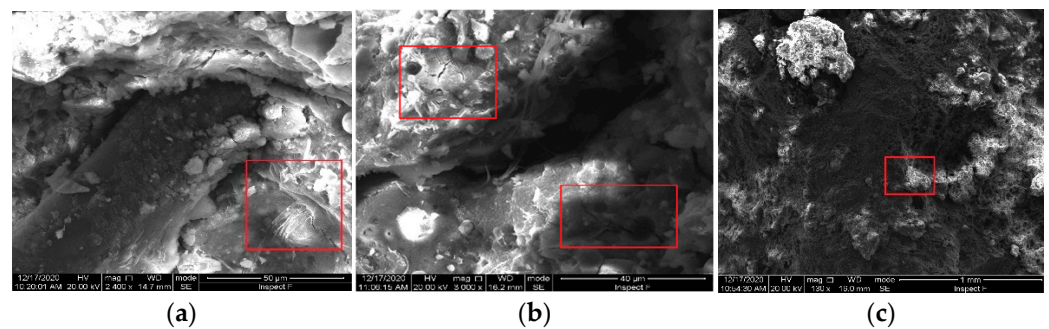


Figure 8. Micro-structure of GPCC: (a) fiber/matrix interface; (b) cement matrix near GHB; (c) GHB/matrix interface.

4. Conclusions

- (1) The content of GHB has a significant effect on the compressive and split tensile strengths and thermal conductivity, the effect of water–cement ratio on split tensile strength is more significant. The PVA content has little effect on the strength and thermal conductivity of GPCC. The optimal ratio was determined as 40% GHB, 1.5% PVA fiber, and 0.26 water-binder ratio.
- (2) In this experiment, when the content of GHB is greater than 40%, there is a significant reduction in strength, and the effect of fiber is not obvious. It may be that the high doping amount of GHB will have interaction with the PVA fiber, and this problem should be considered in the next research.
- (3) The change of the GHB content has a significant effect on the mechanical index and thermal conductivity of GPCC. As the GHB content is increased, the compressive strength and tensile strength gradually decrease, and the thermal conductivity starts

to rise after a significant decreasing trend. Therefore, further optimization of the GHB content can be considered to reduce the thermal conductivity of GPCC and ensure its mechanical properties.

- (4) Through micromechanical analysis, the presence of glass beads reduces the bond between the PVA fiber and the cement matrix, and reduces the role of the fiber in inhibiting the development of cracks. The coexistence of PVA fiber and glass beads in the cementitious materials does not play their respective roles well.

Author Contributions: Conceptualization, J.D.; data curation, X.L.; formal analysis, X.L.; funding acquisition, J.D.; investigation, X.L. and Y.L.; methodology, X.L. and Y.Z.; project administration, X.L.; supervision, Y.Z.; writing—original draft, J.D. and Y.Z.; writing—review and editing, X.L. and Y.L. All authors have read and agreed to the published version of the manuscript.

Funding: This work was financially support by the Henan Key Laboratory of Grain and Oil Storage Facility & Safety (2020KF-B04), application research plan of key scientific research projects for universities in Henan Province (21A560006), the scientific research founding for advance talents of Henan University of Technology (2018BS006). The authors also express their sincere thanks to bachelors Yungeng Wu and Linkai Ma for their experimental support. Additionally, thank you to the Experimental Center of the College of Civil Engineering and Architecture in Henan University of Technology.

Data Availability Statement: The corresponding author will provide the datasets created and analyzed during this study upon reasonable request.

Conflicts of Interest: The authors declare that they have no conflicting financial interests or personal relationships that may have influenced the work presented in this study.

References

- Lee, J.; Wi, S.; Jeong, S.; Chang, S.J.; Kim, S. Development of thermal enhanced n-octadecane/porous nano carbon-based materials using 3-step filtered vacuum impregnation method. *Thermochim. Acta* **2017**, *655*, 194–201.
- Lachheb, M.; Younsi, Z.; Naji, H.; Karkri, M.; Nasrallah, S.B. Thermal behavior of a hybrid PCM/plaster: A numerical and experimental investigation. *Appl. Therm. Eng.* **2017**, *111*, 49–59.
- Dean, B.; Dulac, J.; Petrichenko, K.; Graham, P. *Towards Zero-Emission Efficient and Resilient Buildings*; Global Status Report; Global Alliance for Buildings and Construction (GABC): Paris, France, 2016.
- Ari, I.; Sari, R. Differentiation of developed and developing countries for the Paris Agreement. *Energy Strategy Rev.* **2017**, *18*, 175–182.
- Aghniaey, S.; Lawrence, T.M. The impact of increased cooling setpoint temperature during demand response events on occupant thermal comfort in commercial buildings: A review. *Energ. Build.* **2018**, *173*, 19–27.
- Xu, X.; Zhong, Z.; Deng, S.; Zhang, X. A review on temperature and humidity control methods focusing on air-conditioning equipment and control algorithms applied in small-to-medium-sized buildings. *Energ. Build.* **2018**, *162*, 163–176.
- Yao, W.; Pang, J. Performance degradation and microscopic structure of glazed hollow bead insulation normal concrete after exposure to high temperature. *Acta Mater. Compos. Sin.* **2019**, *36*, 2932–2941.
- Zhang, Y.; Ma, G.; Liu, Y.; Li, Z. Mix design for thermal insulation concrete using waste coal gangue as aggregate. *Mater. Res. Innov.* **2015**, *19*, S5–S878.
- Zhao, L.; Wang, W.; Li, Z.; Chen, Y.F. An experimental study to evaluate the effects of adding glazed hollow beads on the mechanical properties and thermal conductivity of concrete. *Mater. Res. Innov.* **2015**, *19*, S5–S929.
- Liu, J.; Liu, Y.; Feng, D. Effect of reinforcement ratio on seismic performance of thermal insulation concrete shear wall with glazed hollow bead. *Eng. J. Wuhan Univ.* **2017**, *50*, 269–273.
- Feng, W. Study on Flexural Behavior of Glazed Hollow Bead Insulation Concrete Beams. Master's Thesis, Taiyuan University of Technology, Taiyuan, China, 2015.
- Zhu, B.; Han, L. Aseismic structure design of glazed hollow bead insulation concrete shear wall. *China Earthq. Eng. J.* **2018**, *40*, 963–968.
- Chang, J. Research on Thermal Performance of Thermal Insulation Glazed Hollow Bead Concrete Hollow Shear Walls. Master's Thesis, Taiyuan University of Technology, Taiyuan, China, 2015.
- Wu, D. Bearing Capacity of Glazed Hollow Bead Insulation Concrete Beams and Columns after Exposure to Elevated Temperatures. Master's Thesis, Taiyuan University of Technology, Taiyuan, China, 2013.
- Wu, H. Vitriified Microsphere, the Performance Analysis of External Thermal Insulation Walls. Master's Thesis, Hunan University of Science and Technology, Xiangtan City, China, 2017.

16. Zhu, J.; Li, G. Performance of thermal insulation materials of polypropylene fiber reinforced vitrified small ball. *J. Build. Mater.* **2015**, *18*, 658–662.
17. Wu, W.J.; Yu, Y.M. Study on proportioning of vitrified beads insulation mortar based on single factor analysis. *Mater. Rep.* **2014**, *28*, 385–390.
18. Lim, Y.; Li, V.C. Durable repair of aged infrastructures using trapping mechanism of engineered cementitious composites. *Cem. Concr. Compos.* **1997**, *19*, 373–385.
19. Parra-Montesinos, G.; Wight, J.K. Seismic response of exterior RC column-to-steel beam connections. *J. Struct. Eng.* **2000**, *126*, 1113–1121.
20. Li, V.C.; Wu, C.; Wang, S.; Ogawa, A.; Saito, T. Interface tailoring for strain-hardening polyvinyl alcohol-engineered cementitious composite (PVA-ECC). *Mater. J.* **2002**, *99*, 463–472.
21. Shao, Y.; Shah, S.P. Mechanical properties of PVA fiber reinforced cement composites fabricated by extrusion processing. *Mater. J.* **1997**, *94*, 555–564.
22. Li, V.C.; Wang, S.; Wu, C. Tensile strain-hardening behavior of polyvinyl alcohol engineered cementitious composite (PVA-ECC). *Mater. J.* **2001**, *98*, 483–492.
23. Lye, H.L.; Mohammed, B.S.; Liew, M.S.; Wahab, M.; Al-Fakih, A. Bond behaviour of CFRP-strengthened ECC using Response Surface Methodology (RSM). *Case Stud. Constr. Mater.* **2020**, *12*, e327.
24. Al-Fakih, A.; Mohammed, B.S.; Liew, M.S. On rubberized engineered cementitious composites (R-ECC): A review of the constituent material. *Case Stud. Constr. Mater.* **2021**, *14*, e536.
25. Research of the Properties of Polyvinyl Alcohol Fiber Concrete. Master's Thesis, Yangzhou University, Yangzhou, China, 2018.
26. Meng, Q.; Wang, D.; Liu, Z. Performance analysis of polypropylene fiber mortar in vitrified microspheres. *Build. Energy Effic.* **2017**, *45*, 45–46.
27. Feng, T.; Xu, L.; Shi, X.; Han, J.; Zhang, P. Investigation and Preparation of the Plastering Mortar for Autoclaved Aerated Blocks Walls. *Crystals* **2021**, *11*, 175.
28. Fan, S.; Wang, P.; Liu, Z. Drying shrinkage and cracking behavior of polypropylene fiber reinforced glazed hollow beads thermal insulation mortar. *J. Build. Mater.* **2017**, *20*, 118–123.
29. Xu, J.; Liu, Y.; Liu, Z.Q. Test research of steel fiber insulation concrete compressive performance. *Concrete* **2014**, *11*, 93–95.
30. Wang, C. Effect of Polyvinyl Alcohol Fiber and Vitrified Micro Bead On Properties of Foam Concrete. Master's Thesis, Inner Mongolia University of Science and Technology, Baotou, Inner Mongolia, China, 2019.
31. GB/T 50081; Standard for Test Method of Mechanical Properties on Ordinary Concrete. Beijing Standards Press of China: Beijing, China, 2019.
32. GB/10295; Standard for Thermal Insulation—Determination of Steady-State Thermal Resistance and Related Properties—Heat Flow Meter Apparatus. Beijing Standards Press of China: Beijing, China, 2008.